Journal of Alloys and Compounds 509 (2011) 7657–7661

Contents lists available at ScienceDirect

Journal of Alloys and Compounds

journal homepage: www.elsevier.com/locate/jallcom

Thermodynamic and kinetic analysis for carbothermal reduction process of CoSb alloy powders used as anode for lithium ion batteries

Jianying Yang[a], Mengwei Wang[a], Yuntong Zhu[b], Hailei Zhao[a,c,*], Ronglin Wang[a], Jingbo Chen[a]

[a] School of Material Science and Engineering, University of Science and Technology Beijing, Beijing 100083, China
[b] Tsinghua High School, Beijing 100084, China
[c] Beijing Key Lab of New Energy Material and Technology, Beijing 100083, China

ARTICLE INFO

Article history:
Received 15 January 2011
Received in revised form 28 April 2011
Accepted 30 April 2011
Available online 10 May 2011

Keywords:
Carbothermal reduction
Synthesis
CoSb
Anode
Lithium ion battery

ABSTRACT

Thermodynamic calculation and kinetic analysis were performed on the carbothermal reduction process of Co_3O_4–Sb_2O_3–C system to clarify the reaction mechanism and synthesize pure CoSb powder for the anode material of secondary lithium-ion batteries. The addition of carbon amount and thus the purity of CoSb powders were critical to the electrochemical property of CoSb anode. It was revealed that in an inert atmosphere, Co_3O_4 was preferentially reduced to CoO, followed by the reduction of Sb_2O_3 and CoO. CO_2 was the gas product for the reduction of Co_3O_4 and Sb_2O_3, while CO was the gas product for that of CoO. Based on the analysis result, pure CoSb powder without any oxides and residual carbon was synthesized, which showed a higher specific capacity and a lower initial irreversible capacity loss, compared to CoSb sample with residual carbon. This work can be a reference for other carbothermal reduction systems.

1. Introduction

Secondary lithium-ion battery plays more and more important roles in modern society as an energy storage device and is widely used in cell phones, portable electronic devices and electric vehicles. Graphite is the commonly used anode materials for lithium-ion batteries due to its long cycle life, abundant material supply and relatively low cost [1]. However, the relatively low theoretical capacity (372 mAh/g) and the safety issue related to lithium deposition have limited the development of higher performance lithium-ion batteries. Meanwhile, alloy anodes have been considered as one of the most promising electrode materials for the next-generation lithium-ion batteries due to their high energy densities, relatively low cost, environmental compatibility and safe operation potential [2]. They have been attracting lots of attentions and various endeavors have been made aiming to synthesize high performance alloy anode materials [3–13]. Among those different types of candidates for anode materials, Sb-based alloy anode materials have high specific capacity and elevated operating voltage, which can overcome the drastic volume change of metallic antimony during the lithiation and delithiation cycles by introducing less active or inactive component as matrix for active Sb, such as Co [14,15], Se [16], Al [17], Zn [18,19], Ni [20] and Cu [21,22]. Active elements such as Sn [23,24] and In [25] can also make the volume change of the Sb-based electrode take place much smoothly because the lithiation and delithiation of the two active components occur at different potentials, the unreacted phase can accommodate the mechanical strain yielded by the reacted phase.

There are diversified methods for synthesizing Sb-based alloy materials, including mechanical alloying of metal powders [26,27], hydrothermal method [28], chemical precipitation [23,29], electrochemical deposition [30,31] as well as carbothermal reduction of metal oxides [32–35]. Compared to other preparation methods, carbothermal reduction method is low cost and much more easily mass-productive, making it a promising method for both laboratory scale experiment and industrial production. In carbothermal reduction processes, the carbon amount is a critical factor because it determines the purity of the product directly. If the carbon amount is in excess, there will be a certain amount of carbon remained in the synthesized anode materials; on the contrary, less carbon than needed will lead to the incomplete reduction of metal oxides. Either of them will affect the electrochemical properties of materials. Most researches in this field [33,36–40] have been carried out based on the hypothesis that all the carbon is oxidized to CO during the carbothermal process. Nevertheless, the generation of CO_2 cannot be excluded in some systems. Whether CO or CO_2 is possibly produced depends mainly on the chemical features of different metal oxides. As a matter of fact, in a multiple metal oxides carbothermal reduction process, the gas products might be the mixture of

* Corresponding author at: School of Materials Science and Engineering, University of Science and, Technology Beijing, Beijing 100083, China.
E-mail address: hlzhao@ustb.edu.cn (H. Zhao).

0925-8388/$ – see front matter © 2011 Elsevier B.V. All rights reserved.
doi:10.1016/j.jallcom.2011.04.143

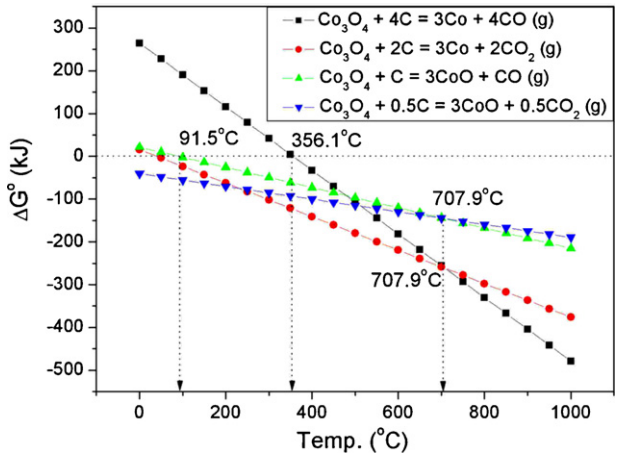

Fig. 1. Gibbs free energies (ΔG^0) of reactions (1)–(4) as a function of temperature.

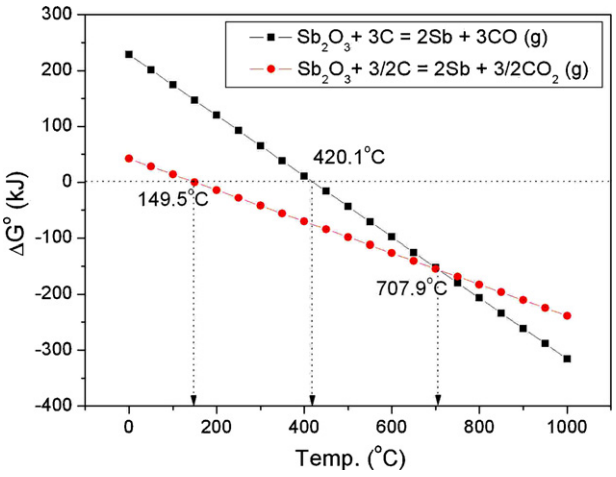

Fig. 3. Gibbs free energies (ΔG^0) of reactions (7) and (8) as a function of temperature.

CO and CO_2 due to various factors. It is of great importance to get further understandings about the carbothermal reduction process details such as the reduction order and the CO and CO_2 composition in the gas product, which can help to determine the precise carbon amount actually required, leading to products of high purity.

In present work, CoSb alloy was selected as an example to clarify the actual kinetic process of carbothermal reduction from Co_3O_4 and Sb_2O_3, based on the thermodynamic analysis of all possible reactions in this system, the SEM observation and chemical composition analysis of the products. With the calculated carbon amount, high purity CoSb alloy were synthesized and its electrochemical property was evaluated and compared with that containing a certain amount of remaining carbon.

2. Thermodynamics analysis

2.1. Co_3O_4–C system

For the carbothermal reduction of Co_3O_4, there is a series of possible reactions. Co_3O_4 can be reduced by carbon directly to metal Co, as described by reactions (1) and (2), or to CoO first and then to Co, as presented by reactions (3)–(6). For each route, the gas product could be CO or CO_2. The standard Gibbs free energies of reactions (1)–(6) as a function of temperature were calculated and plotted in Figs. 1 and 2. With respect to the thermodynamic calculation, the standard enthalpies and entropies at different temperatures for different species were looked up from handbooks [41,42], then the enthalpy change (ΔH_T^0) and the entropy change (ΔS_T^0) at different temperatures for a certain reaction could be derived. Accordingly, the standard Gibbs free energies at different temperatures for a certain reaction could be calculated by the equation of $\Delta G_T^0 = \Delta H_T^0 - T\Delta S_T^0$.

From the perspective of thermodynamics, reactions (2) and (4) are more feasible compared to reactions (1) and (3) below 707.9 °C, i.e. CO_2 will be produced as gas product. With respect to reactions (2) and (4), the latter is even easier to occur at low temperature. According to Fig. 2, CoO can be reduced by carbon to metal Co via reactions (6) or (5) at the temperature below or above 707.9 °C, respectively.

$$Co_3O_4 + 4C = 3Co + 4CO(g) \quad (1)$$

$$Co_3O_4 + 2C = 3Co + 2CO_2(g) \quad (2)$$

$$Co_3O_4 + C = 3CoO + CO(g) \quad (3)$$

$$Co_3O_4 + 0.5C = 3CoO + 0.5CO_2(g) \quad (4)$$

$$CoO + C = Co + CO(g) \quad (5)$$

$$CoO + 0.5C = Co + 0.5CO_2(g) \quad (6)$$

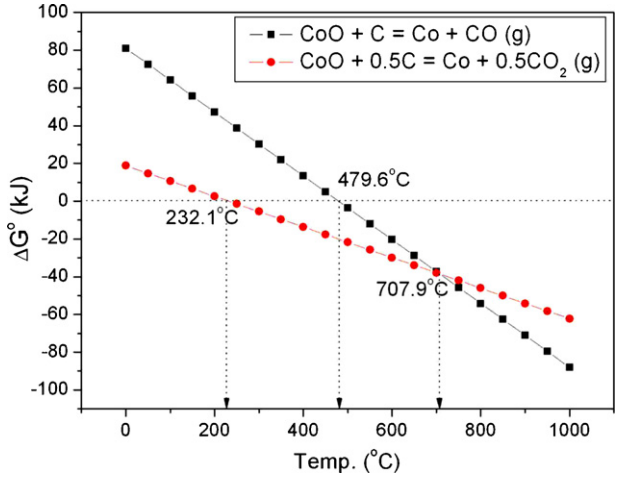

Fig. 2. Gibbs free energies (ΔG^0) of reactions (5) and (6) as a function of temperature.

2.2. Sb_2O_3–C system

The possible reactions for the carbothermal reduction of Sb_2O_3 are reactions (7) and (8), corresponding to the generation of CO and CO_2 gases, respectively. Fig. 3 shows the Gibbs free energies of reactions (7) and (8) as a function of temperature [41,42], indicating their theoretical feasibility when temperature is above 420.1 °C and 149.5 °C, respectively. At temperature lower than 707.9 °C, reaction (8) has a lower Gibbs free energy value.

$$Sb_2O_3 + 3C = 2Sb + 3CO(g) \quad (7)$$

$$Sb_2O_3 + 3/2C = 2Sb + 3/2CO_2(g) \quad (8)$$

According to the above analyses, it can be concluded that CO_2 gas will be the reduction product if the temperature is lower than 707.9 °C, otherwise CO gas will be.

2.3. Co–Sb system

Our previous work on the thermodynamic calculation [33] indicated that the alloying reaction of Co with Sb (reaction (9)) could occur in the temperature range from 0 to 1000 °C. It is worth to note that the alloying reaction (9) is an exothermic reaction, which

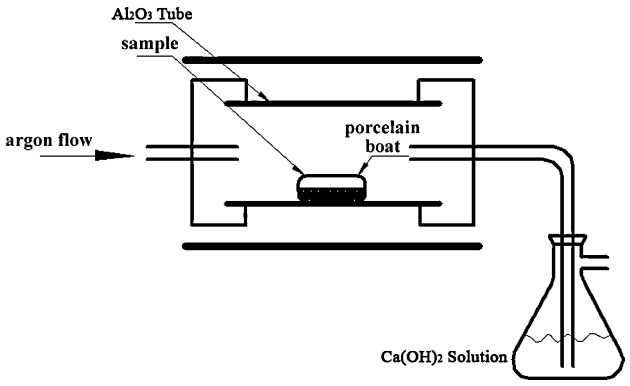

Fig. 4. Schematic drawing of the setup for CO_2 analyzing.

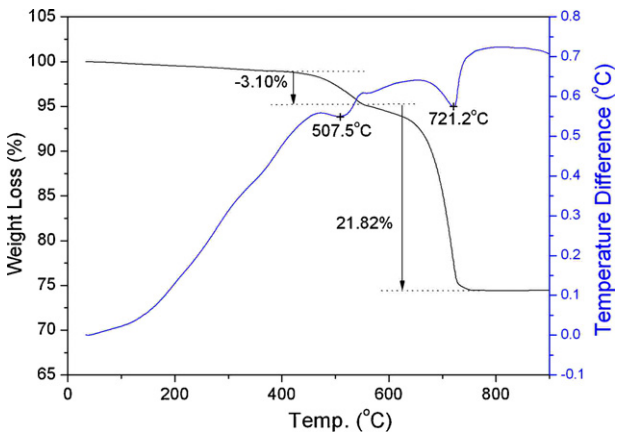

Fig. 5. TG-DTA curves of Co_3O_4–Sb_2O_3–C system with the molar ratio of 3:2:17.

has a positive effect for the endothermic carbothermal reduction process of the metal oxides.

$$Co + Sb = CoSb \quad (9)$$

3. Experimental

Co_3O_4, Sb_2O_3 and carbon were used as raw materials in present work. Those three different powders were mixed and ground in an agate mortar following different stoichiometric ratios. The mixed powders were put into a temperature-controlled tubular furnace equipped with flowing argon and calcined at 800 °C for 2 h. The products were removed from the off-powered furnace after cooling down naturally to room temperature.

Thermo-gravimetric/differential thermal analysis (TG-DTA, NETZSCH STA 449 C) was conducted with a heating rate of 5 °C/min under a N_2 flux of 40 ml/min. The phases of carbothermal reduction product were analysed by X-ray Diffraction (XRD) over the 2θ range from 10 to 90° using a Rigaku D/max-A diffractometer with Cu Kα radiation (40 kV, 100 mA). The microstructure of synthesized alloy powders was observed by scanning electron microscope (SEM, LEO-1450).

The CO_2 amount in the gas product of the carbothermal reduction was determined with a self-fabricated device as depicted in Fig. 4. The sample was calcined in a tube furnace under flowing argon. The produced gases with the flowing argon were vented into $Ca(OH)_2$ solution, where CO_2 gas could be absorbed and $CaCO_3$ precipitation was formed. After washing, filtering and drying, the $CaCO_3$ precipitation was weighed and accordingly the CO_2 amount could be derived.

Li/$LiPF_6$ (EC + DMC)/CoSb two-electrode half-cells were assembled for cycling tests. Firstly, CoSb electrode was prepared using the synthesized CoSb powders mixed with acetylene black as conductive additive and polyvinylidene fluoride (PVDF) as binder, which was dissolved in *N*-methyl-pyrrolidinone in the weight ratio of 80:10:10 and then painted on a copper foil used as current collector. Then the electrode was pressed and dried at 120 °C under vacuum for 24 h. Lastly, cells were assembled in an argon-filled glove box using Celgard 2400 polyethylene as separator, 1 M $LiPF_6$ in a mixture of ethyl carbonate (EC) and dimethyl carbonate (DMC) (1:1 in vol. ratio) as electrolyte, and metallic lithium foil as counter electrode. The cycling tests were carried out at current density of 100 mA/g in voltage range of 0.01–1.5 V versus Li/Li^+ by LAND BT-10 tester (Wuhan, China).

4. Results and discussion

In order to gain an insight into the kinetic process of CoSb alloy via carbothermal reaction, TG-DTA analysis was performed on Sb_2O_3–Co_3O_4–C powders, which was prepared in the molar ratio of Sb_2O_3:Co_3O_4:C = 3:2:17 according to reaction (10), where carbon monoxide (CO) was supposed to generate during the carbothermal reduction process, and the carbon amount in reaction (10) was defined as full carbon. The TG-DTA result was shown in Fig. 5. Before 420 °C, the system had a little mass loss, which corresponded to the vaporization of water contained in the slightly damped raw materials. From 420 to 550 °C, the system underwent a process with a mass loss of 3.10 wt% (first step), accompanied with an endothermic peak centered at ca. 507.5 °C. After 550 °C, there was a slow weight loss and then followed by a rapid loss from 650 to 720 °C with an endothermic peak at ca. 721.2 °C. The total weight loss in 550–720 °C was 21.82 wt% (second step).

To determine the reduction sequence of these oxides or the actual kinetic process of the carbothermal reduction, the theoretical mass losses of the carbothermal reduction of different oxides via the generation of CO_2 or CO gases, respectively, were calculated based on the total loaded material weight. The results were listed in Table 1. It was apparent that the weight loss of 3.10 wt% between 420 and 550 °C was ascribable to the reduction of Co_3O_4 to CoO, as described in reactions (3) or (4). Considering the thermodynamic analysis in Section 2, reaction (4) was preferable below 707.9 °C. With respect to the weight loss of 21.82 wt% produced in 550–720 °C, it should be associated with the reductions of Sb_2O_3 and CoO. The thermodynamic calculation (Figs. 2 and 3) suggested that Sb_2O_3 was relatively easier to be reduced by carbon compared to CoO. Because the second weight loss process started below 707.9 °C, it was reasonable to state that the reduction of Sb_2O_3 was via the route of reaction (8). For the reduction of CoO, either reaction (5) or reaction (6) was possible, as the reduction process lasted to 720 °C. If CoO was reduced via reaction (5), then the whole weight loss of the second step was (12.50 + 10.37) = 22.87 wt%, theoretically. Meanwhile, if it was reduced via reaction (6), then the whole weight loss should be (12.50 + 8.46) = 20.96 wt%. The actual weight loss in this period (21.82 wt%) was just in between.

$$3Sb_2O_3 + 2Co_3O_4 + 17\,C \rightarrow 6CoSb + 17CO(g) \quad (10)$$

Then, we can deduce that the reduction process could carry out via the routes of reactions (4), (5) and (8) or (4), (6) and (8). The former route corresponded to the whole reaction (11), while the latter to the reaction (12). Compared to the required amount of carbon for reaction (10), where all oxides were supposed to be oxidized via the generation of CO gases, the carbon amount required for the accomplishment of reactions (11) and (12) were only 67.7% and 50% of the full carbon, respectively. With the help of the setup described in Fig. 4, the produced CO_2 amount was calculated, which was much closer to the theoretical result predicted by reaction (11). Accordingly, reaction (11), consisting of reactions (4), (5) and (8), was the most possible route for the carbothermal reduction synthesis of CoSb alloy powders.

$$3Sb_2O_3 + 2Co_3O_4 + 23/2\,C \rightarrow 6CoSb + 6CO(g) + 11/2CO_2(g) \quad (11)$$

Table 1
Theoretical mass loss* corresponding to the carbothermal reduction of different oxides via the generation of CO_2 or CO gases, respectively.

	$Co_3O_4 \rightarrow CoO$		$CoO \rightarrow Co$		$Sb_2O_3 \rightarrow Sb$	
	CO_2	CO	CO_2	CO	CO_2	CO
Weight loss (wt%)	2.82	3.59	8.46	10.37	12.50	16.15

* Based on the total loaded material weight as expressed in reaction (10).

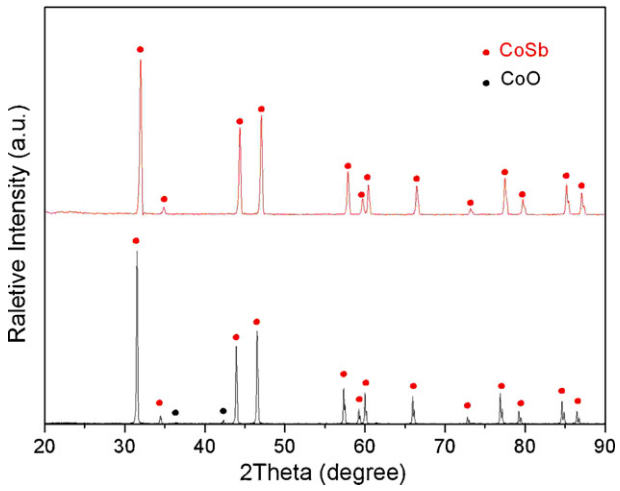

Fig. 6. XRD patterns of the samples with 60% and 65% of full carbon amount.

$$3Sb_2O_3 + 2Co_3O_4 + 17/2\,C \rightarrow 6CoSb + 17/2CO_2(g) \quad (12)$$

In order to verify the theoretically predicted result, two Sb_2O_3–Co_3O_4–C samples with 60% and 65% of the full carbon were prepared and calcined at 800 °C for 2 h in flowing Ar atmosphere, respectively. The XRD patterns of the synthesized materials are shown in Fig. 6. For sample with 60% C, besides the peaks to CoSb, a little amount of impurity was detected, which could be assigned to CoO, indicating that the reduction of oxides was not complete and the carbon amount was insufficient. Fortunately, all the peaks of sample with 65% C were identified as CoSb and no other impurity or residual carbon was detected. This is well consistent with the theoretically predicted result.

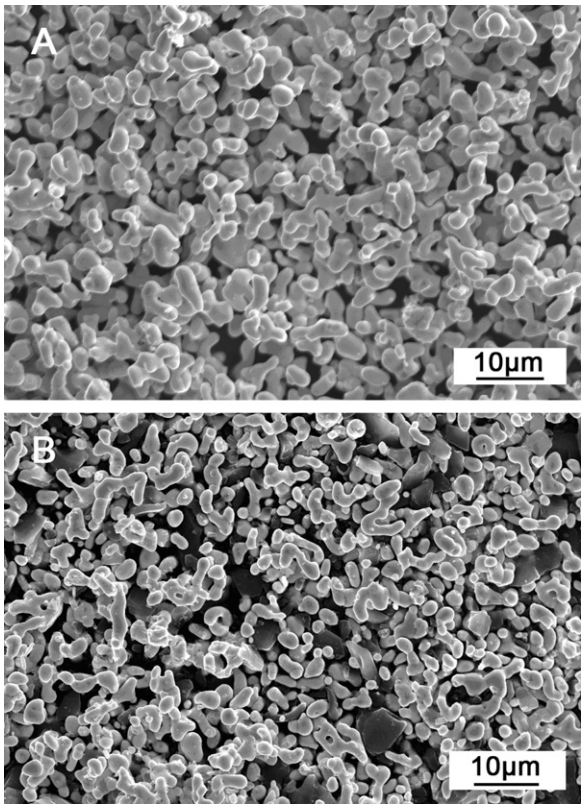

Fig. 7. SEM images of the synthesized powders. (A): 65% carbon; (B): full carbon.

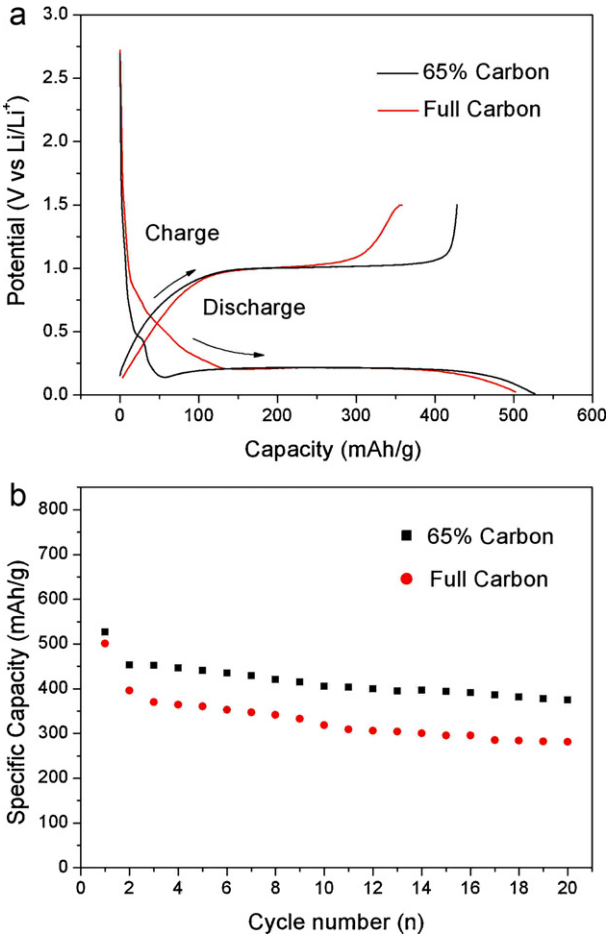

Fig. 8. Electrochemical performance of CoSb powder synthesized from 65% carbon and full carbon prescription: (a) potential profiles; (b) cycling performance.

SEM observation was performed on the synthesized CoSb powders prepared from 65% and 100% of full carbon, respectively. Fig. 7 presents the SEM images of two samples. Sample with 65% C showed worm-like particle morphology without observable carbon component, i.e. pure CoSb alloy powders, while sample with 100% C displays mixture morphology with relatively smaller CoSb alloy particles and irregular carbon particles, i.e. CoSb/C composite powders.

The electrochemical property of the two samples as anode material for lithium ion battery was evaluated by two-electrode method. The samples were cycled at 100 mA/g between 0.01 and 1.5 V versus Li/Li^+. As illustrated in Fig. 8(a) and (b), CoSb electrode presented a higher reversible capacity and a lower initial irreversible capacity loss than CoSb/C electrode, which can be attributed to the high purity of the CoSb sample. The residual carbon in the CoSb/C sample should be responsible for its lower specific capacity. The synthesized pure CoSb alloy exhibited a specific capacity of ca. 400 mAh/g, which was much higher than that of the commonly used graphite anode materials, and thus being a promising anode material for lithium ion battery.

5. Conclusions

The kinetic process of carbothermal reduction of Co_3O_4–Sb_2O_3–C system was investigated with the aim of understanding the detailed process and synthesizing pure CoSb alloy powders. The thermodynamic calculation and the TG-DTA analysis revealed that Co_3O_4 was preferentially reduced to CoO at relatively

lower temperature, then followed by the simultaneous reduction of Sb_2O_3 and CoO by carbon. The former is reduced by carbon via the generation of CO_2 gases, while the latter is reduced via the formation of CO gases. The overall reaction for the synthesis of CoSb alloy from Co_3O_4–Sb_2O_3–C system could be expressed as: $3Sb_2O_3 + 2Co_3O_4 + 23/2\,C \rightarrow 6CoSb + 6CO\ (g) + 11/2CO_2\ (g)$, which was verified by the actual experiments. Based on this result, pure CoSb alloy powders were synthesized, which exhibited a higher reversible capacity and a lower initial capacity loss, compared with the carbon-containing CoSb samples. The kinetic analysis is of great importance to the synthesis of desired materials.

Acknowledgements

This research work has been performed with the financial support of 863 Program of National High Technology Research Development Project of China (no. 2006AA43Z231), Program for Guangdong Industry-Academy-Alliance Research (no. 2009A090100020) and Program for New Century Excellent Talents in University of China (no. NCET-07-0072).

References

[1] W. Zhang, J. Power Sources 196 (2011) 13.
[2] W. Zhang, J. Power Sources 196 (2011) 877.
[3] H. Sakaguchi, H. Honda, Y. Akasaka, T. Esaka, J. Power Sources 119–121 (2003) 50.
[4] W. Pu, X. He, J. Ren, C. Wan, C. Jiang, Electrochim. Acta 50 (2005) 4140.
[5] Q. Li, S. Hu, H. Wang, F. Wang, X. Zhong, X. Wang, Electrochim. Acta 54 (2009) 5884.
[6] X. Wang, Z. Wen, Y. Liu, X. Wu, Electrochim. Acta 54 (2009) 4662.
[7] B. Das, M.V. Reddy, P. Malar, T. Osipowicz, G.V. Subba Rao, B.V.R. Chowdari, Solid State Ionics 180 (2009) 1061.
[8] X. Fan, F. Ke, G. Wei, L. Huang, S. Sun, J. Alloys Compd. 476 (2009) 70.
[9] S. Liu, Q. Li, Y. Chen, F. Zhang, J. Alloys Compd. 478 (2009) 694.
[10] J. Li, J. Swiatowska, A. Seyeux, L. Huang, V. Maurice, S. Sun, P. Marcus, J. Power Sources 195 (2010) 8251.
[11] J. He, H. Zhao, J. Wang, J. Wang, J. Chen, J. Alloys Compd. 508 (2010) 629.
[12] Y. Lin, J. Duh, H. Sheu, J. Alloys Compd. 509 (2011) 123.
[13] A.N. Jansen, J.A. Clenenger, A.M. Baebler, J.T. Vaughey, J. Alloys Compd. 509 (2011) 4457.
[14] C.M. Ionica, P.E. Lippens, J.O. Fourcade, J.-C. Jumas, J. Power Sources 146 (2005) 478.
[15] C.H. Mi, Y.X. Cao, X.G. Zhang, H.L. Li, Solid State Commun. 149 (2009) 781.
[16] M. Xue, Z. Fu, J. Alloys Compd. 458 (2008) 351.
[17] M. Stjerndahl, H. Bryngelsson, T. Gustafsson, J.T. Vaughey, M.M. Thackeray, K. Edstrom, Electrochim. Acta 52 (2007) 4947.
[18] X.B. Zhao, G.S. Cao, Electrochim. Acta 46 (2001) 891.
[19] G.S. Cao, X.B. Zhao, T. Li, C.P. Lu, J. Power Sources 94 (2001) 102.
[20] J. Xie, X.B. Zhao, H.M. Yu, H. Qi, G.S. Cao, J.P. Tu, J. Alloys Compd. 441 (2007) 231.
[21] J. Ren, X. He, W. Pu, C. Jiang, C. Wan, Electrochim. Acta 52 (2006) 1538.
[22] M. Morcrette, D. Larcher, J.M. Tarascon, K. Edstrom, J.T. Vaughey, M.M. Thackeray, Electrochim. Acta 52 (2007) 5339.
[23] Z. Wang, W. Tian, X. Li, J. Alloys Compd. 439 (2007) 350.
[24] F. Wang, M. Zhao, X. Song, J. Alloys Compd. 472 (2009) 55.
[25] A.J. Kropf, H. Tostmann, C.S. Johnson, J.T. Vaughey, M.M. Thackeray, Electrochem. Commun. 3 (2001) 244.
[26] H. Honda, H. Sakaguchi, Y. Fukuda, T. Esaka, Mater. Res. Bull. 38 (2003) 647.
[27] E. Ronnebro, J. Yin, A. Kitano, M. Wada, T. Sakai, Solid State Ionics 176 (2005) 2749.
[28] Z. Wang, W. Tian, X. Liu, X. Li, J. Solid State Chem. 180 (2007) 3360.
[29] C. Yin, H. Zhao, H. Guo, X. Huang, W. Qiu, J. Univ. Sci. Technol. B 14 (2007) 345.
[30] H. Bryngelsson, J. Eskhult, L. Nyholm, K. Edstrom, Electrochim. Acta 53 (2008) 7226.
[31] L. Huang, X. Zheng, Y. Wu, L. Xue, F. Ke, G. Wei, S. Sun, Electrochem. Commun. 11 (2009) 585.
[32] H. Zhao, D.H.L. Ng, Z. Lu, N. Ma, J. Alloys Compd. 395 (2005) 192.
[33] M. Wang, H. Zhao, J. He, R. Wang, J. Chen, N. Chen, J. Alloys Compd. 484 (2009) 864.
[34] H. Zhao, C. Yin, H. Guo, J. He, W. Qiu, Y. Li, J. Power Sources 174 (2007) 916.
[35] H. Zhao, Z. Zhu, C. Yin, H. Guo, D.H.L. Ng, Mater. Chem. Phys. 110 (2008) 201.
[36] K. Wang, X. He, J. Ren, L. Wang, C. Jiang, C. Wan, Electrochim. Acta 52 (2006) 1221.
[37] J. He, H. Zhao, M. Wang, X. Jia, Mater. Sci. Eng. B 171 (2010) 35.
[38] H. Guo, H. Zhao, C. Yin, W. Qiu, J. Alloys Compd. 426 (2006) 277.
[39] H. Guo, H. Zhao, X. Jia, W. Qiu, F. Cui, Mater. Res. Bull. 42 (2007) 836.
[40] H. Guo, H. Zhao, X. Jia, J. He, W. Qiu, X. Li, J. Power Sources 174 (2007) 921.
[41] M.W. Chase, Jr. J. Physical Chemical Reference Data, NIST-JANAF Thermochemical Tables, Fourth ed., Monograph No. 9 (1998).
[42] J.A. Dean, Lange's Handbook of Chemistry, Fifteenth ed., 1998.